

Feasibility study of fault rupture deviation by slurry wall

M. Fadaee¹, M.K. Jafari^{2,*}, M. Kamalian³, A. Shafiee⁴, S.M. Moosavi⁵

Received: 2012/12/17, Revised: 2013/04/13, Accepted: 2013/07/15

Abstract

During past earthquakes, many instances of building damage as a result of earthquake surface fault rupture have been observed. The results of investigating a potential mitigation scheme are presented in this paper. Such plan provides a wall in the soil with the aim of surface displacement localization in the narrow pre-determined location. This may reduce the risk of the future rupture downstream the wall. To evaluate the efficiency of the method, this paper (i) provides validation through successful class "A" predictions of 1g model tests for fault deviation by weak wall; and (ii) conducts sensitivity analyses on fault position, fault offset and wall shear strength. It is shown that wall can be designed to deviate rupture path; even downstream of the wall can be protected.

Keywords: Reverse fault rupture, Soil bentonite wall, Fault deviation.

1. Introduction

During past earthquakes, surface rupture has caused devastation of numerous structures like buildings, bridges, pipelines. Following the two major earthquakes in Turkey and Taiwan in 1999 and collapse of many structures due to fault rupture, serious attention was paid to this subject. The length of causative fault of Chi-Chi earthquake in Taiwan (1999) is about 90 km. This fault speeded all the way to the ground surface. The severe tectonic deformation caused a variety of structural failures, and well-documented case histories of fault rupture interaction with engineering structures [1,2]. Another example is Wenchuan 2008 earthquake with magnitude of Mw 7.9 which occurred along the Longmenshan fault, a thrust structure along the border of the Indo-Australian plate and Eurasian plate. As shown in Figure 1a, the road offsets vertically by 2 m and the buildings next to the right side of the road collapsed. Figure 1b, shows a school, whose left side was driven 2 m upward and the building was largely undamaged [3]. This photo shows that in some circumstances, the rupture can be deviated from the structure.

A wide variety of studies were carried out worldwide on the subject of fault rupture emphasizing on the three fields: (a) analysis of case histories [4,2,5,6], (b) physical modeling studies [7,8,9,10] and (c) numerical or analytical studies [11,12,13].

The main concern of aforementioned studies is to investigate the influential parameters of fault rupture-structure interaction. To take this problem into account, most seismic design codes prevent construction across, or in the immediate vicinity of seismically active faults. For instance, the Alquist-Priolo earthquake fault zoning Act and Part 5 of Eurocode 8 prohibit construction in fault setback. However, determination of fault setback is very difficult, since only in a few regions a trustful mapping of seismically active faults can be found. In addition to the uncertainty related to the mapping of active faults, in many cases there exist secondary faults with the associated ruptures located at relatively large distances from the main trace of the faults. Several examples are reported for the aforementioned earthquakes, where most ground distortion took place in an area some tens of meters wide, but extensional cracks were also observed several hundreds of meters from the main trace. In Landers earthquake, around 45% of all surface ruptures fell outside the setback determined from Alquist-Priolo fault zoning [15].

Therefore, in cases where there is a significant degree of uncertainty in the fault mapping, and the risk induced by secondary ruptures cannot be avoided, structural or geotechnical engineering countermeasure are needed to reduce the hazard. As structural point of view, utilization of rigid foundation systems to resist the induced stresses due to

* Corresponding Author: jafari@iiees.ac.ir

¹ PhD, Research Assistant, International Institute of Earthquake Engineering and Seismology (IIEES)

² Professor of Geotechnical Engineering Research Center, International Institute of Earthquake Engineering and Seismology (IIEES)

³ Associate Professor of Geotechnical Engineering Research Center, International Institute of Earthquake Engineering and Seismology (IIEES)

⁴ Research fellow, Civil engineering department, UCLA

⁵ Assistant Professor, Mazandaran University



Fig. 1 Reverse fault rupture examples during the 2008 Wenchuan earthquake in China (a) The road offset vertically by 2m and buildings to the right of the road collapsed, b) The yard of Bailu middle school was offset vertically by 2 m and the building are largely undamaged . [photos adapted from reference 3]

the excessive ground displacements would be beneficial. The foundation's position relative to the free field reverse fault trace as well as its bearing pressure, consist two of the most important parameters that control the surface fault rupture-foundation interaction. Figure 2 presents different fault rupture-foundation interaction. Three mechanisms can happen depending on the relative position of foundation to the fault break, alluvium depth and foundation bearing pressure. In mechanisms "A" and C, the rupture diverts toward the hanging wall or footwall due to the presence of a heavy bearing

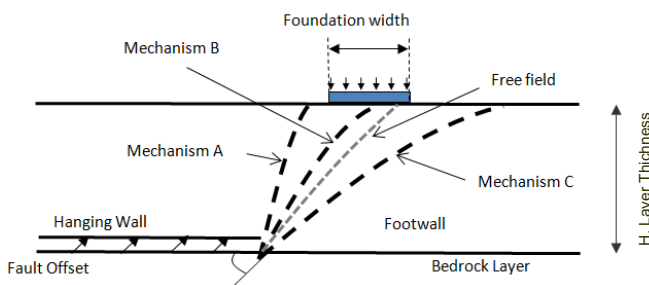


Fig. 2 Different fault rupture foundation interaction: Mechanism A: rupture is diverted to the hanging wall, Mechanism B: rupture hits the foundation, and Mechanism C: rupture is diverted to the footwall

pressure, whilst, in the mechanism B, rupture hits the foundation [10,16]. Some analytical studies have suggested a minimum weight of the structure required to divert fault rupture beneath the foundation [17,18]. On the other hand, geotechnical point of view might involve the use of ductile compacted fill or reinforced fill. These efforts have focused on spreading out the surface fault displacement to a wider zone. To this end, installing geogrid, have been investigated [19].

In the case of new structures, although a rigid and continuous foundation system or using geogrid can easily be applied for, it is not that simple for the retrofitting of existing structures. Especially for historic buildings and monuments, these methods may be practically impossible. Even if avoidance could be an option for new structures, for existing structures and monuments another solution may be adopted. Especially for the historic buildings and monuments, minimum intervention is quite desirable.

As it was discussed previously, the rupture can be deviated by the presence of heavy structure. The purpose of this paper is to investigate the applicability of rupture deviation using a weak vertical element in soil to localize fault displacement in a pre-determined narrow zone. The underlying idea is briefly addressed in Figure 3a. As can be observed, the free-filled surface fault displacement and the corresponding shear band propagate in alluvium depending on the type, dip, and displacement of fault; nevertheless, in Figure 3b, by constructing a wall with lower shear strength compared to the alluvium, the rupture is localized in the weak zone. In other words, downstream of the wall protected.

The question raised is, what technique for construction of the weak wall should be used, and which material is appropriate for filling it up. The results of the present study suggest that soil bentonite wall can be a proper candidate in this regard. Soil-bentonite wall is constructed by backfilling a trench with a mixture of soil, bentonite, and water (Figure 4). Trench is stabilized while being filled with slurry. The

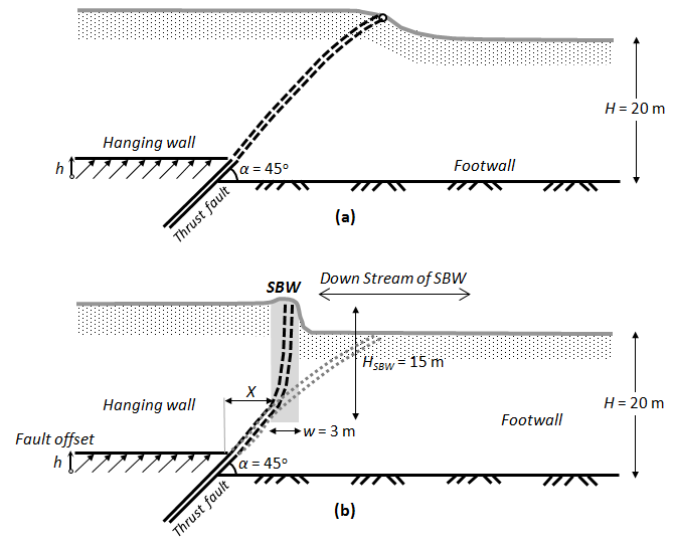


Fig. 3 Problem definition and geometry: (a) Thrust fault rupture, propagating through a 20 m high alluvium, (b) placement of soil bentonite wall (SBW) leads to fault rupture diversion and mitigation of the hazard



Fig. 4 The view of construction of soil bentonite soil bentonite wall a) Excavation of trench in the soil under presence of bentonite b) mixing the soil with bentonite and pouring again in the trench c) top view of excavated soil bentonite wall [photos adapted from reference 20]

other end of the trench is backfilled with soil-bentonite while the excavation proceeds along one end of the trench. An important usage of such a wall is to create a low-permeable diaphragm in subsurface to limit or direct the underground flow. It can be used to control the seepage flow under embankment dams as well as landfill leakages. [20,21].

By using this type of wall and applying the numerical and experimental methods, the present research aims to show that by constructing a soil bentonite wall the future fault rupture deviate into the wall and downstream of the wall is protected from future hazard.

2. Modelling Techniques

In the present study, 1g physical modelling tests as well as numerical FEM analyses were carried out in order to investigate the soil bentonite wall effects on fault rupture propagation paths. To ensure that the numerical model could reveal reasonable predictions, physical sandbox model experiments were carried out. A small 1:100-scale model was first built as a physical model. Then, the results of the physical model test were compared with those produced by numerical analyses to ensure the correctness of the numerical simulation.

The full-scale numerical model was then adopted to

reproduce the deformational behavior of the overburden soil when it is subjected to the reverse faulting caused by an earthquake.

2.1. Physical modelling techniques

1g physical modelling tests were carried out in this study in order to better understand the soil bentonite wall's effects on the fault rupture propagation path through the alluvium. The 1g model testing gives good insight to the problem of fault rupture and it has been used by the past researchers [9,22,23]. Lee and Hamada (2005) compared the result of 1g and centrifuge model testing and concluded that the result of 1g testing would be reliable at least in qualitative manner.

The dimensions of the used sandbox apparatus in the tests are 110 cm in length, 60 cm in height, and 50 cm in width. The length of mobile hanging wall is 40 cm. A schematic view of faulting apparatus along with its picture is shown in Figure 5. The footwall length is selected to be 70 cm to minimize the side boundary effects on the results.

The system utilizes an electric motor, and has been designed to model reverse and normal fault rupture events along different dip angles. The tests examined reverse fault rupture propagation with a dip angle of 45 degrees through the bedrock in a quasi- static mode.

The Firoozkooh sand (No.161) with a mean grain size (D_{50}) of 0.25 mm was used in the present study as the alluvium where faulting passes through. Figure 6 presents the grain size distribution curve of the sand. The specific gravity, minimum and maximum dry density of the aforementioned sand are 2.61, of 1.71 g/cm³ and 1.42 g/cm³, respectively. The sand was poured into the box with a pre-defined height and velocity to achieve a relative density of approximately 55% which represents a medium loose state for all the tests (Figure 7).

As stated previously, the SBW is a mixture of soil, bentonite,

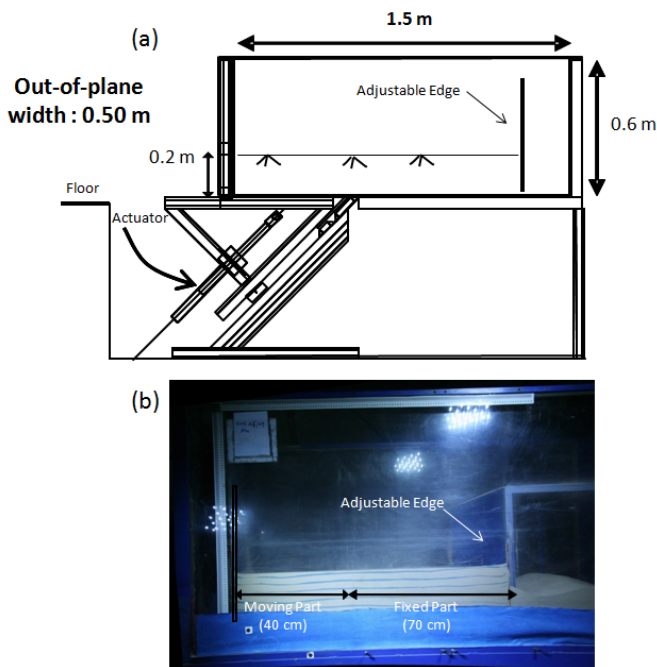


Fig. 5 The 1g faulting apparatus (a) schematic view of test apparatus (b) photo of the fault box

and water. In our 1g models, to satisfy the scale rule, (To have low enough shear strength and high enough compressibility), a mixture of kaolinite, bentonite, and water is used.

To install the wall, first, two steel plates are placed in the box at the desired locations. Then, the sand is poured to the required depth (i.e. 5cm). Next, the clay slurry is poured between the two plates and the rest of the box filled with the sand. Finally, two plates are extracted carefully.

Two plexiglass plates were placed at each face of the box, perpendicular to the fault strike to facilitate digital photography all through the model. The displacement field in the scaled model experiments was constantly monitored using high-resolution optical image correlation techniques. Such optical strain monitoring quantifies the spatial pattern of strain accumulation in the tests. Digital images of the soil sample were captured using a digital camera with 8 million pixels resolution placed in front of the 1g test apparatus. A series of digital images were collected as the faulting tests proceeded in each 2mm base dislocation. Each picture corresponded to a different fault displacement. An optical flow program was written in order to measure soil displacement by comparing sequences of the digital images captured in time. Post

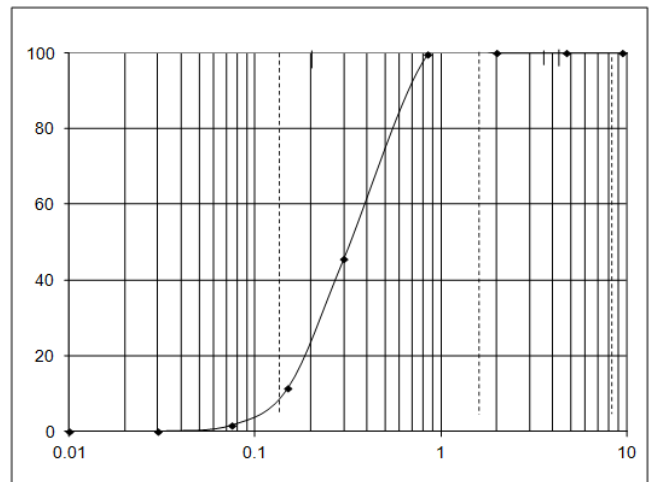


Fig. 6 Grain size distribution curve of the Firoozkooh sand



Fig. 7 The sand raining bucket and the fault rupture box

processing allowed examination of the displacement and strain fields. Validation of image processing program was also carried out to ensure acceptable results. For instance, comparison of foundation rotation, measured by the electronic device above the foundation, with that of the image processing technique showed a satisfactory (Figure 8). A comprehensive description of the image processing technique from camera calibration to the results validation can be found in Fadaee et.al 2013 [23].

2.2. Finite element modelling (FEM)

The main role of FEM in this study is to observe the differences between surface profiles and rupture path with and without wall. Despite its unavoidable shortcomings, FE modelling has been shown to be capable of efficiently reproducing fault rupture propagation in the free field [11,22] as well as its interaction with surface foundations [24]. An essential requirement is to adopt a refined mesh and an appropriate constitutive model for soil [22]. For this purpose, the commercial FE code ABAQUS (2011) was used. The soil is modeled with quadrilateral continuum elements of dimension $d_{FE} = 0.5$ m to achieve a reasonably refined mesh. An elasto-plastic isotropic strain softening constitutive model with Mohr-Coulomb failure criterion was adopted [11]. Strain softening is introduced by reducing the mobilized friction angle φ_{mob} and the mobilized dilation angle ψ_{mob} with the increase of plastic octahedral shear strain :

$$\varphi_{mod} = \left\{ \begin{array}{l} \varphi_p - \frac{\varphi_p - \varphi_{res}}{\gamma_f^p} \gamma_{oct}^p, \text{ for } 0 \leq \gamma_{oct}^p < \gamma_f^p \\ \varphi_{res} \quad \quad \quad \text{for } \gamma_{oct}^p \geq \gamma_f^p \end{array} \right\} \quad (1)$$

$$\psi_{mod} = \left\{ \begin{array}{l} \psi_p \left[1 - \frac{\gamma_{oct}^p}{\gamma_f^p} \right], \text{ for } 0 \leq \gamma_{oct}^p < \gamma_f^p \\ \psi_{res} \quad \quad \quad \text{for } \gamma_{oct}^p \geq \gamma_f^p \end{array} \right\} \quad (2)$$

where : φ_p and φ_{res} are the peak mobilized friction angle and its residual (or critical state) value ; ψ_p is the peak dilation angle ; γ_f^p is the plastic octahedral shear strain at the end of softening. Pre-yield behavior is modeled as linear elastic, with a secant elastic modulus linearly increasing with depth in full scale model.

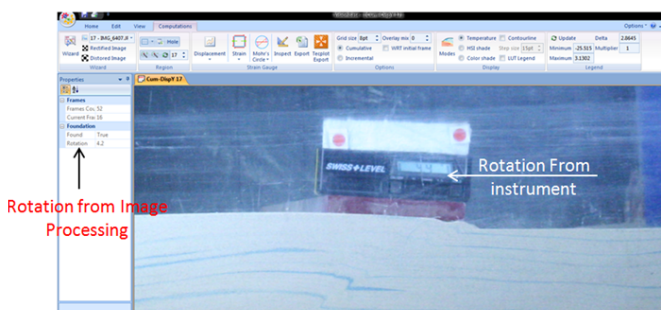


Fig. 8 Validation of image processing program performance by comparison of foundation rotation from instrument and program

Two kind of numerical models for the free field fault rupture analyses are used: a) small scale numerical model which represents the 1g tests), and b) full scale model (Figure 9). Small scale numerical model is used to calibrate numerical model and verify the effectiveness of proposed method. Then, on the basis of this model, full scale numerical model is built.

To obtain material property of the soil in 1g test (Model a) and prototype condition (Model b), direct shear tests on sand and clay were run. To model a 20 m alluvium depth, Normal stress (σ_v) varied from 100 to 400 kPa, and to model 1g model tests, σ_v was kept less than 10 kPa. When $\sigma_v \geq 100$ kPa, the peak and residual friction angles were $\varphi_{peak} = 32^\circ$ and $\varphi_{res} = 30^\circ$. On the other hand, for low normal stress ($\sigma_v < 10$ kPa), the peak friction angle increases substantially, reaching $\varphi_{peak} \approx 45$. Although this soil is in loose state, in very low normal stress, it can dilate and show peak and post peak behavior [25,28].

The numerical model (which was extensively used in QUAKER project [11,24]) is capable to reproduce soil behavior by a series of FE simulations of the direct shear test. In this simulation, all soil parameters including elastic (or deformation) modulus were determined.

For estimation of soil bentonite wall (SBW) property in prototype scale, according to the literature [26,27], it may be conservatively assumed that the final undrained shear strength (S_u) can be estimated on the basis of normally consolidated samples. Based on the results of triaxial consolidated undrained (CU) tests of such samples, combined with the empirical correlations of S_u with PI and OCR [28], the normalized undrained shear strength of the clay mixture was estimated as $S_u / \sigma_v' = 0.25$. A secant Young modulus $E/S_u = 300$ was also considered suitable for the clay.

In 1g small-scale model testing, an extensive effort was devoted to find an appropriate clay, so that its strength remains constant during the test, or it should show a very low rate of consolidation. A mixture of three parts of kaolinite to one part of montmorillonite (based on dry weight) was selected appropriate after a survey of a range of clay mixtures. The mixture exhibits a low rate of consolidation, and has a LL of 110% and a PL of 25%.

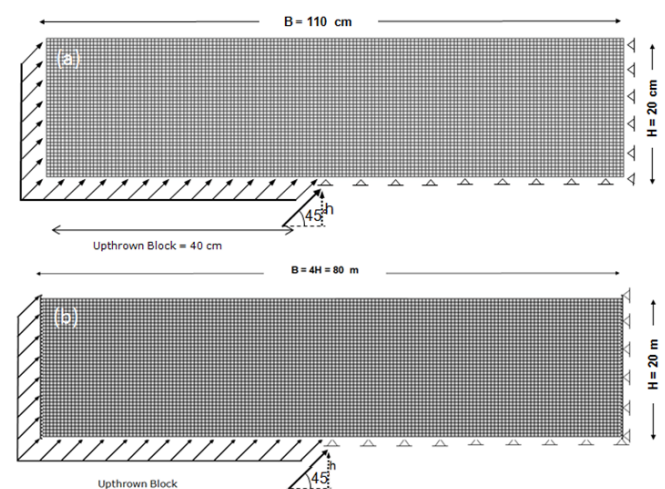


Fig. 9 Mesh, Geometry and boundary condition of fault rupture model a) small-scale numerical model representative for the 1g tests, b) full scale numerical model

Various water contents resulted in different undrained shear strength of clay. The undrained shear strength of the model clay was adjusted by changing the model clay's water content. The water content of the model clay was selected to be 100% which corresponds to an undrained shear strength of 1.2 kPa.

Prior to imposing fault displacement, the in situ stresses were allowed to develop by standard boundary conditions. Then, the fault displacement was monotonically applied through the left side and the left bottom boundaries of the model, while other boundaries were kept fixed. The large displacement Lagrangian description was adopted in numerical analyses because of the large imposed displacement.

3. Reduced 1g Model Results

3.1 Free-field fault rupture propagation

Results from the free field test are discussed first as a reference. The deformed soil model (Figure 10a) with superimposed displacement vectors (as computed through image processing) is compared with the FE deformed mesh, for bedrock fault offset $h = 1$ m. However, we applied $h=1$ cm to the

model, to maintain a 1:100 scale: all 1g test results are presented in prototype. The analysis appears to agree qualitatively with the experiment, predicting with reasonable accuracy the rupture path and the location of its emergence at the ground surface.

This is further confirmed in Figure 10b, which compares the experimental with the analytical results in terms of vertical displacement profiles at the ground surface, for fault offset amplitude of 1 m. While the analysis results are plotted for $h = 1.0$, the experimental images were obtained for roughly the same bedrock offset $h = 0.95$ m. Due to very low confining pressure, small-scale experiments do offer valuable qualitative insights on the mechanics of rupturing. The only difference refers to the slope of the surface scarp, which appears to be shallower in the numerical model. This discrepancy can be attributed to siding effect, and numerical model simplification.

Siding effect can be seen in Figure 11. Although the plexiglass is considered to be smooth to reduce the friction with soil, the fault outcrop is not still linear. On the other hand, the numerical model can capture the main mechanism of the fault rupture, however, still some differences exist even in class "A" prediction of centrifuge modelling due to the simplified modelling of post-peak soil behavior [24].

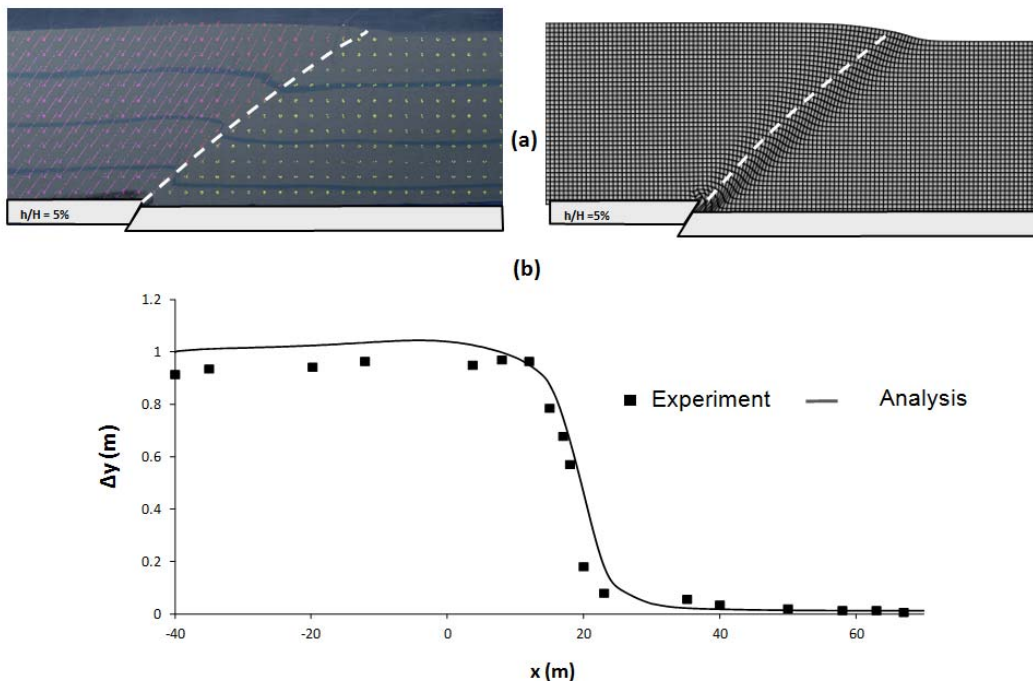


Fig. 10 Free-field thrust fault rupture propagation through loose sand. Comparison of experimental with numerical analysis results: (a) photo of the deformed model with superimposed displacement vectors computed through image analysis, compared to FE deformed mesh with superimposed shear strain for bedrock fault offset $h = 1$ m; (b) vertical displacement profiles at the soil surface for fault offset of 1m

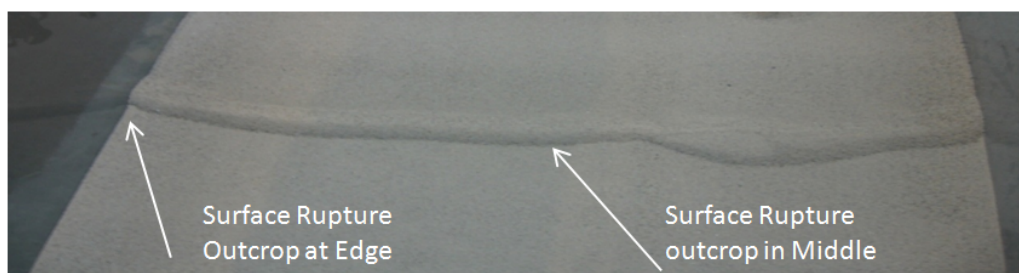


Fig. 11 Top view of the surface rupture outcrop in 1g test

3.2 Results for free field fault rupture in treated case

In the second step, the results for the case of fault diversion by addition of a wall is investigated. SBW thickness (w) is 3m, positioned at a distance of 8 m from the hanging-wall as shown in Figure 12. Again image of the deformed soil with superimposed displacement vectors (Figure 12a) is compared with the FE deformed mesh, for bedrock fault offset $h = 1$ m. As seen, a good estimation was made by the numerical analysis to capture main behavior of the experiment.

A comparison of surface profile between the experiment and numerical model was made in Figure 12b for abovementioned fault offset. The maximum vertical displacement in the wall vicinity is larger in the numerical model, but are identical at

other areas. This inconsistency can be attributed to the difference in clay behavior, since the clay in the experiment tends to behave in a more ductile manner. Despite this qualitative difference, the numerical and experimental results are comparable in terms of surface profile. The SBW manages to deviate most of the faulting-induced shear band effectively towards the wall.

The magnitude of fault offset is important parameter in fault rupture problems. To investigate the influence of this parameter the test was continued by imposing more displacement on the hanging wall. A picture of the deformed model with superimposed displacement vectors computed through image analysis and top view of the first and second rupture on the surface are shown in Figure 13 when the fault

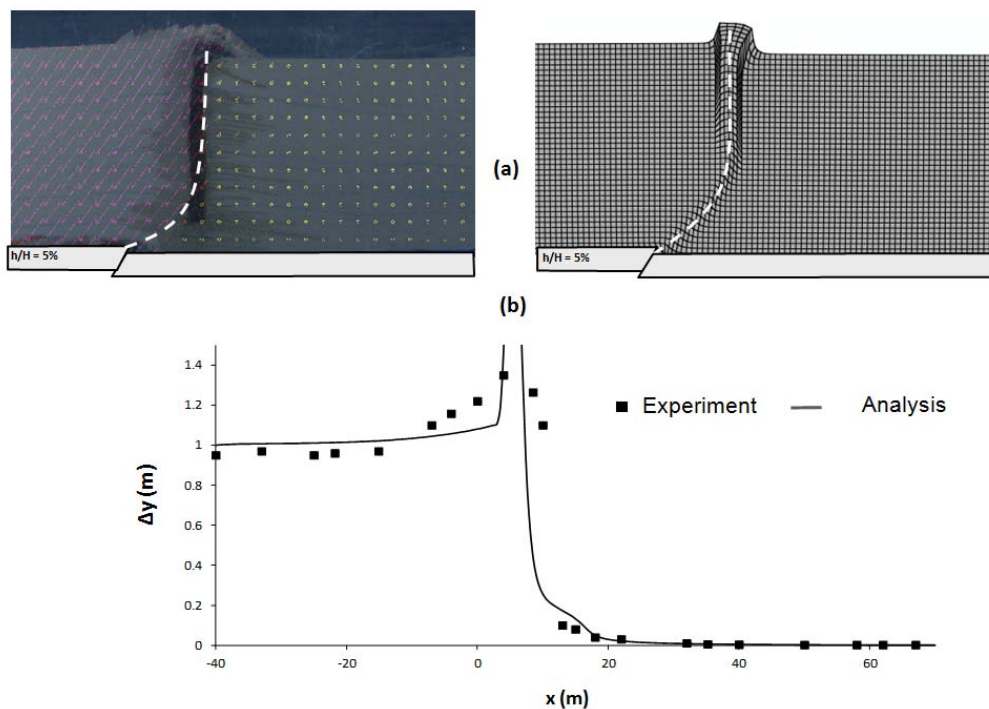


Fig. 12 Interaction of a reverse fault rupture propagating through loose sand with soil bentonite wall (SBW) positioned at $X = 8$ m; comparison of experimental with numerical analysis results: (a) photo of the deformed model with superimposed displacement vectors computed through image analysis, compared to FE deformed mesh with superimposed shear strain for bedrock fault offset $h = 1$ m; (b) vertical displacement profiles at the soil surface for fault offset of 1m

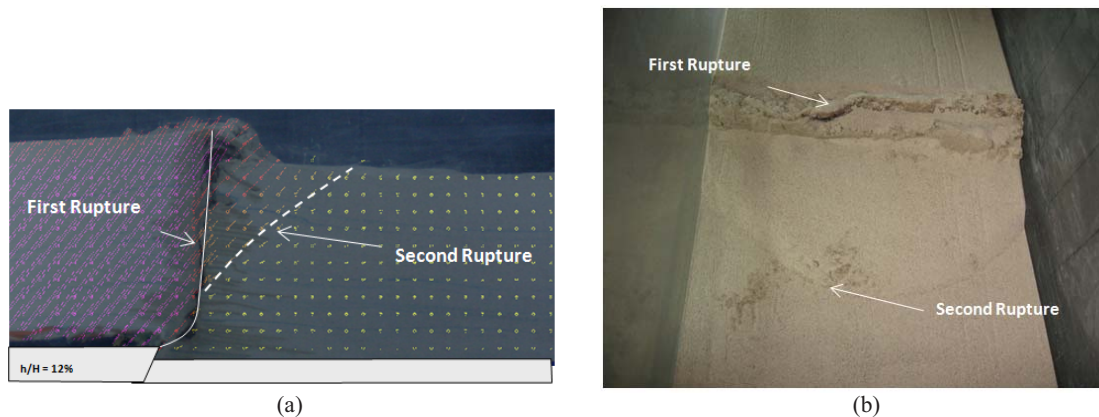


Fig. 13 Fault rupture-SBW interaction mechanisms for fault offset $h=2.4$ m for wall positioned at $x=8$ m in experiment, a) photo of the deformed model with superimposed displacement vectors computed through image analysis ; b) top view of the first and second rupture on the surface

offset (h) reached 2.4 m. As can be seen, there are two rupture paths, one in the SBW and another one which starts from a depth of 13 m and continues towards the downstream of the wall. The second rupture path outcrop on the surface is clear in the top view of the fault box in Figure 13b. In the numerical model similar results were obtained at least qualitatively. The secondary rupture is created when the fault offset reached 2 m. In Figures 14a and 14b the deformed mesh and vertical surface profile are shown. Although 1 m fault offset rupture path diverted in the wall completely, in 2 m fault offset a secondary rupture is created. In the numerical model, secondary rupture created in smaller fault offset comparing to the 1g model test. This discrepancy can be attributed to the difference in clay behavior, since the clay in the experiment is more compressible than numerical model. Despite this qualitative difference, both the numerical and experimental results show creation of secondary rupture. It appears that, to maintain full absorption of the fault offset, a thicker wall or two walls will be required to accommodate the larger lateral compressional deformation.

4. Discussion

A study on the influence of fault break position and shear strength of the soil bentonite wall has been conducted incorporating a full scale numerical model (Figure 9b) to obtain a perspective of the fault rupture propagation pattern through the sand layer in the presence of soil bentonite wall.

4.1 Fault break position

As it was discussed previously, precise determination of fault break is difficult in many situations. In many cases, instead of introducing a single line for fault location, the fault zone can be determined. Intersection of rupture path with SBW is necessary

for its deviation. Hence, for proper design of the wall depth, a numerical sensitivity analysis is needed. In other words, analyses should be repeated for a range of postulated possible fault break positions and dips. Through such analysis, appropriate wall depth can subsequently be determined according to different possible fault outcrop. For instance, a parametric study on the effect of the location of the fault rupture relative to the wall is presented in Figure 15. As seen, in the three fault break locations (Figs. 15 b, c, d and e), SBW succeeded to attract the rupture toward itself. In Figure 11e although the rupture has not been diverted completely, the area which intended to protect from rupture remain almost intact and the secondary rupture passes through downstream of the wall. The surface profile of the three aforementioned fault breaks for the case of with and without wall are compared in Figure 16. For different fault breaks, the surface profile is shifted from left to the right from $x=15$ to $x=0$ m. However, when the wall is constructed in front of the possible fault break,

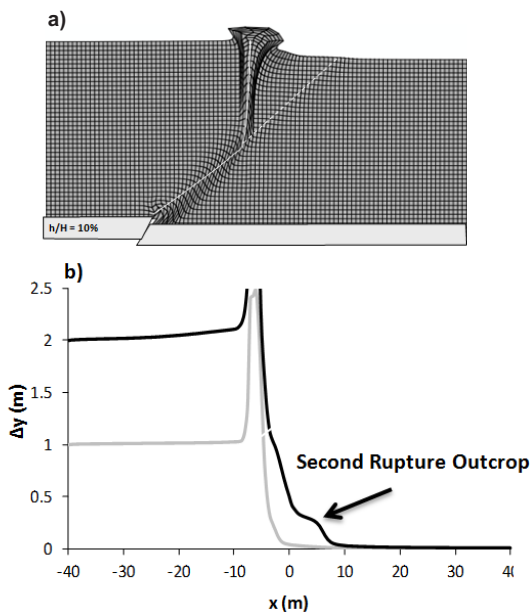


Fig. 14 Numerical model of fault rupture-SBW interaction mechanisms for fault offset $h=2.0$ m for wall positioned at $x=8$ m, (a) the deformed mesh with superimposed shear strain (b) comparison of vertical surface profile for two different fault offset

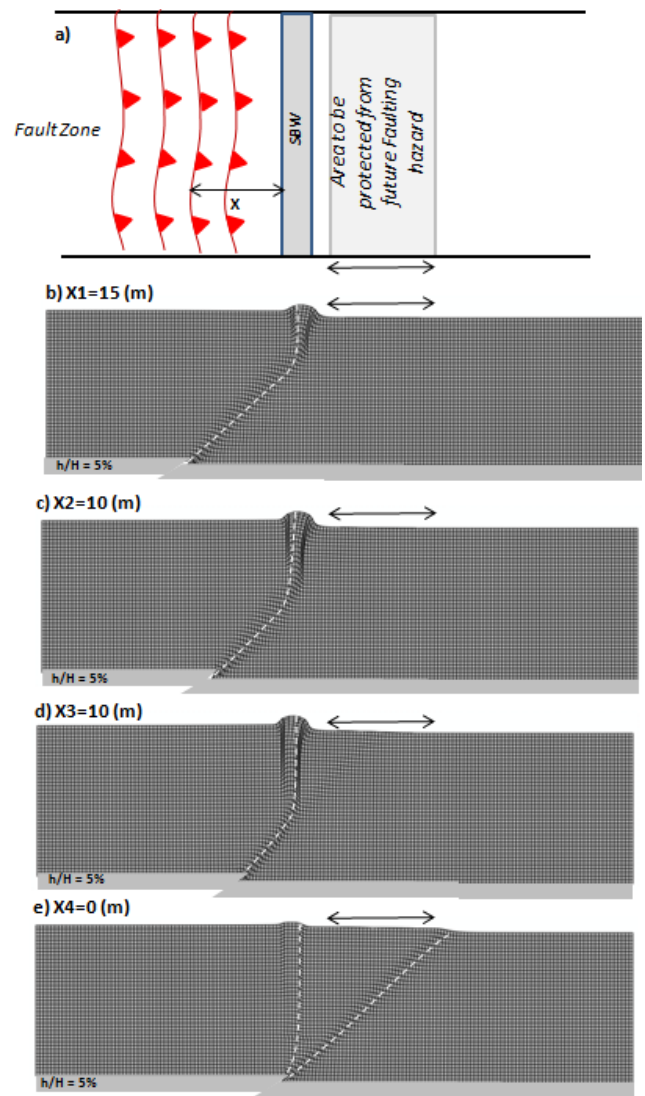


Fig. 15 An arbitrary problem definition and geometry: wall thickness=3m, alluvium thickness=15m : (a) plan of the problem showing different fault locations and placement of soil bentonite wall (SBW) for protection of specific area. (b), (c), (d) and (e) deformed mesh with superimposed shear strains for three different fault locations (X)

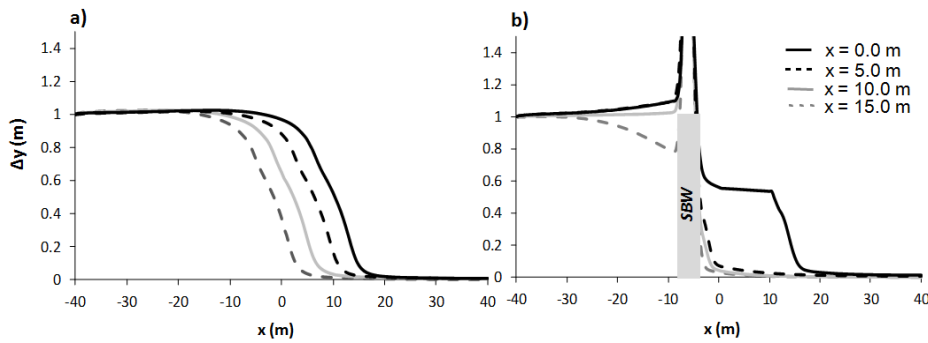


Fig. 16 Comparison of vertical surface profile for three different fault break position $X=15$, 10 and 5 m propagating through loose sand : (a) free-field reverse fault rupture (b) interaction of a reverse fault rupture with soil bentonite wall (SBW) for bedrock fault offset $h = 1$ m

the surface profile in the protected zone is almost horizontal. It should be mentioned that the wall depth is designed on the basis of possible fault break and the maximum length of area which intended to be protected from future rupture.

4. 2. Shear strength of the soil bentonite wall

Shear strength of the soil bentonite wall comparing to surrounding media is a very crucial parameter. To demonstrate how the shear strength of the soil bentonite wall affects the vertical surface profile, two values of normalized shear strength ($S_u/\sigma'_v=0.25$, and 0.45) have been compared. As shown in Figure 17, the soil bentonite wall with normalized shear strength of 0.25 succeeds to deviate the rupture path. The ground surface displacement shows no remarkable deformation and distortion compared to the zone of distortion in the free field case. Increasing the wall's normalized shear strength to 0.45 reduces the wall's performance significantly. Hence, proper wall's normalized shear strength value should be selected on the basis of the alluvium material to deviate the faulting path inward the wall appropriately.

5. Summary and Conclusion

The main idea of this paper is to make a specific weakness in soil media, the propagation pathway of rupture zone can be diverted toward this area and other areas can be protected from this hazard. The weakness zone can be soil bentonite wall with low shear strength, comparing to alluvium. To investigate the applicability of this method for fault deviation, $1g$ physical

modelling tests were carried out. Then, small-scale numerical model was built and its results were compared to $1g$ tests. It was shown that, the wall can absorb the fault offset due to lower shear strength and higher compressibility regarding to surrounding soil. By applying more fault offset, wall cannot absorb the displacement and secondary rupture created after the wall. Thus, by applying more fault offset, thicker wall may be required to suppress creation of secondary rupture.

Then, full-scale numerical model, is built and influence of fault position and wall shear strength are investigated. As precise determination of fault break is difficult in many situations, analyses should be repeated for a range of postulated possible fault break positions. Through such analysis, suitable wall depth can subsequently be determined according to different possible fault position. Wall's material property should be selected on the basis of surrounding alluvium to deviate the faulting path inward the wall appropriately.

Acknowledgment:The authors would like to acknowledge technical and financial support of IIEES under the research project of " Evaluation of possible measures to construct in vicinity of active fault", and also express their gratitude to the geotechnical earthquake faculty members and physical modelling laboratory staff Mr Shirazian.

References

- [1] Kelson, K.I., Kang, K.-H., Page, W.D., Lee, C.-T., and Cluff, L.S., Representative Styles of Deformation along the Chelungpu Fault from the 1999 Chi-Chi (Taiwan) Earthquake: Geomorphic Characteristics and Responses of Man-made Structures: Bulletin of Seismological Society America, 2001, 91(5), 930-952
- [2] Faccioli E., Anastasopoulos I., Calliero A., and Gazetas G. ,Case histories of fault-foundation interaction, Bulletin of Earthquake Engineering,2008, 6(4),557–583 DOI10.1007/s10518-008-9089-y
- [3] Lin A. ,Ren Z. ,Jia D. ,Wu X. (2009), Co-Seismic Thrusting Rupture and Slip Distribution Produced by the 2008 Mw 7.9 Wenchuan Earthquake, China" Tectonophysics, 2009, 471, 203–215
- [4] Ulusay, R., O. Aydan and M. Hamada ,The Behaviour of Structures Built on Active Fault Zones: Examples from the Recent Earthquakes of Turkey, in Seismic Fault-Induced Failures-Possible Remedies for Damage to Urban Facilities,

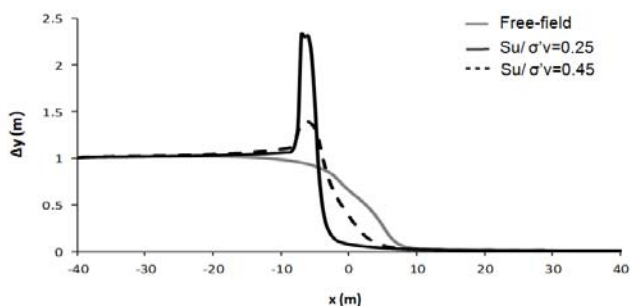


Fig. 17 Influence of wall shear strength on the surface profile compared with free-field condition

- (edited by K. Konagai, University of Tokyo) Japan Soc. Prom. Sci., Japan,2001, pp. 1-26
- [5] Anastasopoulos, I. & Gazetas, G., Foundation-structure systems over a rupturing normal fault: Part I. Observations after the Kocaeli 1999 earthquake, *Bull. Earthquake Eng.*,2007a, 5(5), 253-275.
- [6] Jafari M.K., Moosavi S.M., Lessons to be learned from Surface Fault Ruptures in Iran Earthquakes, Sixth International Conference on Case Histories in Geotechnical Engineering and Symposium in Honor of Professor James K. Mitchell, Arlington, 2008,VA (USA)
- [73] Cole, D. A., Jr. and Lade, P.V., Influence Zones in Alluvium Over Dip-Slip Faults, *Journal of Geotechnical Engineering*, ASCE,1984, 110(5), 599-615.
- [8] Stone, K. J. L. and Wood, D. M., Effects of Dilatancy and Particle Size Observed in Model Tests on Sand, Soils and Foundations, *JSSMFE*,1992, 32(4), 43-57.
- [9] Lee, Jea Woo; Hamada, Masanori, An Experimental Study On Earthquake Fault Rupture Propagation Through A Sandy Soil Deposit, *Structural Engineering / Earthquake Engineering*, 2005, 22(1),1s-13s
- [10] Bransby, M.F., Davies, M.C.R., El Nahas, A., Nagaoka, S., Centrifuge Modelling of Reverse Fault-Foundation Interaction, *Bulletin of Earthquake Engineering*, 2008, 6(4), 607-628
- [11] Anastasopoulos I., Gazetas G., Bransby F., Davies M.C.R., and Nahas El. A., Fault Rupture Propagation through Sand : Finite – Element Analysis and Validation through Centrifuge Experiments, *Journal of Geotechnical and Geoenvironmental Engineering*, American Society of Civil Engineers, (ASCE), 2007, 133(8), 943-958
- [12] Yilmaz MT., Paolucci R., Earthquake Fault Rupture–Shallow Foundation Interaction in Undrained Soils: a Simplified Analytical Approach”, *Earthquake Eng Struct Dyn*, 2007, 36(1),101–118
- [13] Loukidis D, Bouckovalas G, Numerical Simulation of Active Fault Rupture Propagation through Dry Soil, In Proceedings 4th international conference on recent advances in geotechnical earthquake engineering and soil dynamics and symposium in honor of Professor W.D. Liam Finn, San Diego, CA, March,2001, 26–31
- [14] Dong JJ, Wang CD, Lee CT, Liao JJ, Pan YW., The Influence of Surface Ruptures on Building Damage in the 1999 Chi-Chi Earthquake: a Case Study in Fengyuan City. *Engineering Geology* 2004,71,157–179
- [15] Lazarte CA, Bray JD, Johnson AM, Lemmer RE. „Surface Breakage of the 1992 Landers Earthquake and its Effects on Structures, *Bulletin of the Seismological Society of America*,1994, 84:547–561.
- [16] Moosavi, S.M., Jafari, M.K., Kamalian M., Shafiee, A, Experimental Investigation of Reverse Fault Rupture –Rigid Shallow Foundation Interaction, *International Journal of Civil Engineering*,2010, 8(2):85-98
- [17] Paolucci, R., Yilmaz, M.T. „Simplified Theoretical Approaches to Earthquake Fault Rupture-Shallow Foundation Interaction, *Bulletin of Earthquake Engineering*,2008, 6, 629-644.
- [18] Gnajian, N., Fadaee, M, Jafari, M.K, Theoretical and Experimental Approaches to Investigate Earthquake Fault Rupture-Foundation Interaction, 2012,15WCEE Conference on Earthquake engineering, Lisbon, Portugal
- [19] Bray, J.D., "Developing Mitigation Measures for the Hazards Associated with Earthquake Surface Fault Rupture," *Seismic Fault-Induced Failures Workshop*, Japan Society for the Promotion of Science, University of Tokyo, Japan,2001, 55-79. [Invited Paper].
- [20] McKnight, J T Louay M. Owaidat, Quality Control and Performance of a Cut off Wall for Containment of Dnapi Plume, *International Containment & Remediation Technology Conference and Exhibition*, 2001, Orlando, Florida
- [21] Ryan, C, Vertical groundwater barriers for contaminated site reclamation, 2007 Proceedings of the 10th Australia New Zealand Conference on Geo-Mechanics
- [22] Bray JD, The Effects of Tectonic Movements on Stresses and Deformations in Earth Embankments, 1990, Ph.D. thesis, University of California, Berkeley
- [23] Moosavi, S M, Earthquake Fault Rupture Propagation through Soil: Reduction of Seismic Risk through the Application of Geotechnical Engineering Techniques,2010, PhD Thesis, International Institute of seismology and earthquake engineering
- [24] Fadaee, Jafari, M.K., Kamalian, M., Mustafa, S.A, Fault Rupture Propagation in Alluvium and its Interaction with Foundation: New Insights from 1g Modelling via High Resolution Optical Image Processing Techniques, 2013, Vol 14 No 4
- [25] Anastasopoulos I., Antonakos G., Gazetas G., Slab Foundations Subjected to Thrust Faulting: Parametric Analysis and Simplified Design Method, *Soil Dynamics & Earthquake Engineering*, 2010, 30(10), 912–924.
- [26] Fadaee M, Anastasopoulos I., Gazetas G. M.K. Jafari, M. Kamalian, Soil Bentonite Wall Protects Foundation from Thrust Faulting : Analyses and Experiment, 2012, Accepted to the journal of Earthquake Engineering and Engineering Vibration
- [26] Evans, J and Ryan, C. „Time-Dependent Strength Behaviour of Soil-Bentonite Slurry Wall Backfill, 2005, Proceedings of the Sessions of the Geo-Frontiers ASCE Congress January 24–26, Austin, Texas, USA
- [27] Douglas, S. R. Jones, Verification of a Deep Soil-Bentonite Barrier Wall Using the CPTu, Partners Pty Ltd, Newcastle, Australia G. Taylor Austress Menard Pty Ltd, Sydney, Australia, 2010, 2nd International Symposium on Cone Penetration Testing, Huntington Beach, CA, USA, 599-615.
- [28] Look, B. G., *Handbook of Geotechnical Investigation and Design Tables*, 2007, Taylor & Francis Group, London.
- [29] Anastasopoulos, I. Georgarakos, T. Georgiannou, V. Drosos, V. Kourkoulis R. Seismic Performance of Bar-Mat Reinforced-Soil Retaining Wall: Shaking Table Testing versus Numerical Analysis with Modified Kinematic Hardening Constitutive Model, *Soil Dynamics & Earthquake Engineering*, 2010, 30(10), 1089–1105.
- [30] Anastasopoulos I., Gerolymos N., Gazetas G., and Bransby M. F., "Simplified approach for design of raft foundations against fault rupture.Part I: Free-field", *Earthquake Engineering and Engineering Vibration*, Vol.7, pp. 147-163, 2008.
- [31] Anastasopoulos I., Gerolymos N., Gazetas G., and Bransby M. F., "Simplified approach for design of raft foundations against fault rupture.Part II : Soil-Structure Interaction", *Earthquake Engineering and Engineering Vibration*, Vol. 7, pp. 165-179, 2008.